The violation of the Hund rule in semiconductor artificial atoms

2004 Semicond. Sci. Technol. 19 L90

(http://iopscience.iop.org/0268-1242/19/8/L03)

INSTITUTE OF PHYSICS PUBLISHING SEMICONDUCTOR SCIENCE AND TECHNOLOGY

Semicond. Sci. Technol. **19** (2004) L90–L94 PII: S0268-1242(04)76985-0

LETTER TO THE EDITOR

The violation of the Hund rule in semiconductor artificial atoms

C F Destefani[1,2], J D M Vianna[3,4] and G E Marques[2]

[1] Department of Physics and Astronomy, Ohio University, Athens, Ohio 45701-2979, USA
[2] Departamento de Física, Universidade Federal de São Carlos, 13565-905 São Carlos-SP, Brazil
[3] Instituto de Física, Universidade de Brasília, 70910-900 Brasília-DF, Brazil
[4] Instituto de Física, Universidade Federal da Bahia, 40210-340 Salvador-BA, Brazil

Received 2 March 2004
Published 7 July 2004
Online at stacks.iop.org/SST/19/L90
doi:10.1088/0268-1242/19/8/L03

Abstract

The unrestricted Pople–Nesbet approach for real atoms is adapted to quantum dots under applied magnetic field. Gaussian basis sets are used instead of the exact single-particle orbitals in the construction of the appropriated Slater determinants. Both system chemical potential and charging energy are calculated, as well as the expected values for total spin and its z-component. We have verified the validity of the energy shell structure as well as the Hund rule for state population at zero magnetic field. Above given fields, we have observed a violation of the Hund rule by the suppression of triplet and quartet states at the $1p$-energy shell, taken as an example. We have also compared our present results with those obtained by using the **LS**-coupling scheme for low electronic occupations. We have focused our attention on ground-state properties of GaAs quantum dots populated up to 40 electrons.

The influence of spatial confinement on physical properties such as electronic spectra of 0D structures is a topic of growing interest. Among such structures one could select carriers and impurity atoms in metallic or semiconductor mesoscopic structures [1], as well as atoms, ions and molecules trapped into microscopic cavities [1–5]. In these systems, the confinement becomes important whenever a quantum size equals the cavity length. However, the energy spectrum of these systems is not only determined by the spatial confinement and its geometrical shape, but also by environmental facts such as electric and magnetic fields that break or lower general symmetries. Finally, many-body effects such as electron–electron interaction may even be more important than the confinement itself. In any case, a correct description of physical properties of the problem requires that the wavefunction must reflect both the form of the confinement and the appropriated boundary conditions.

Interesting confined systems are the semiconductor quantum dots (QDs), also referred to as artificial atoms, which are built in low-dimensional electronic gases when crystalline translation invariance is broken in all three spatial dimensions; such 3D confinement gives origin to discrete energy states, as it occurs in real atoms. Various are the approaches that have been used to deal with many-particle QDs. Among them, one can cite the charging model [6–9], correlated electron model [10], Green functions [11], Lanczos algorithm [12], Monte Carlo method [13], Hartree–Fock (HF) calculations [14–17], and density functional theory [18]. The charging model, where the electron–electron interaction is assumed as a constant, can reproduce well experimental findings for metallic dots. On the other hand, with much lower electronic density, semiconductor dots require a microscopic point of view to treat the electron–electron interaction.

Here we will consider a QD defined by a hard wall spherical volume, which is more appropriate for semiconductor dots grown inside glass matrices. Some of the commonly studied topics in such systems are the formation of energy shells in their spectra [19], the control of their electronic correlations [20], the formation of Wigner molecules [21], and the influence of the Coulomb interaction in their

spectra [22, 23]. In these spherically defined artificial atoms both spin and orbital angular momenta are good quantum numbers, and the low occupation many-particle eigenstates can be labelled according to the **LS**-coupling scheme [24]. For higher occupation numbers, the **LS**-coupling scheme becomes extremely cumbersome and, because of that, we have chosen to work within the unrestricted Pople–Nesbet matrix approach [25] of the single determinant self-consistent HF formalism; by using it, we were able to treat open and closed shell configurations of QDs containing up to 40 electrons, and the total spin expected values, chemical potential and charging energy could be calculated. We show in this letter the changes induced by the magnetic field on such approach by using a set of Gaussian basis. Then we discuss our main results by focusing on how the magnetic field determines the Zeeman splitting and induces violation of the Hund rule in the population of the QD levels.

Within the unrestricted Hartree–Fock formalism (UHF), the α (spin-up) and β (spin-down) spin orbitals $\chi_i(\mathbf{x})$ may have different spatial components, that is, $\chi_i(\mathbf{x}) = \left\{\psi_j^{\alpha}(\mathbf{r})\alpha(\omega), \psi_j^{\beta}(\mathbf{r})\beta(\omega)\right\}$, where the respective spatial orbitals are $\left\{\psi_j^{\alpha}\middle| j = 1, \ldots, k\right\}$ and $\left\{\psi_j^{\beta}\middle| j = 1, \ldots, k\right\}$. Therefore, an UHF wavefunction has the general form $|\Psi^{\mathrm{UHF}}\rangle = \left|\psi_1^{\alpha}\overline{\psi}_1^{\beta}\cdots\right\rangle$ (the upper bar means spin-down), which represents open shell configurations once no spatial orbital can be doubly occupied. The closed shell solutions can also be obtained [25]; however, UHF functions are not necessarily system eigenstates having well-defined L and S values. Yet, the number of carriers N must equal the sum of spin-up and spin-down electrons, given as $N = N^{\alpha} + N^{\beta}$. The integration of the spin degrees of freedom [25] in this approach yields two coupled HF equations that must be simultaneously solved. They have the form $f^{\alpha/\beta}\left|\psi_j^{\alpha/\beta}\right\rangle = \varepsilon_j^{\alpha/\beta}\left|\psi_j^{\alpha/\beta}\right\rangle$, where the respective Fock operators are given by

$$f^{\alpha/\beta} = h_j + \sum_a^{N^{\alpha/\beta}}\left[J_a^{\alpha/\beta} - K_a^{\alpha/\beta}\right] + \sum_a^{N^{\beta/\alpha}} J_a^{\beta/\alpha}. \tag{1}$$

Both f^{α} and f^{β} include kinetic (h_j), direct $\left(J_a^{\alpha/\beta}\right)$ and exchange $\left(K_a^{\alpha/\beta}\right)$ terms between electrons with same spin, and also a direct term $\left(J_a^{\beta/\alpha}\right)$ between electrons with opposite spin. The interdependence among $f^{\alpha}(f^{\beta})$ and $\psi_j^{\beta}\left(\psi_j^{\alpha}\right)$ requires the simultaneous solution of the two HF equations. They yield the sets $\left\{\psi_j^{\alpha}\right\}$ and $\left\{\psi_j^{\beta}\right\}$ that should minimize the energy E_0^{UHF} of the unrestricted ground-state, $\left|\Psi_0^{\mathrm{UHF}}\right\rangle$, given by

$$E_0^{\mathrm{UHF}} = \sum_a^{N^{\alpha}} h_{aa}^{\alpha} + \sum_a^{N^{\beta}} h_{aa}^{\beta} + \frac{1}{2}\sum_a^{N^{\alpha}}\sum_b^{N^{\alpha}}\left[J_{ab}^{\alpha\alpha} - K_{ab}^{\alpha\alpha}\right] + \frac{1}{2}\sum_a^{N^{\beta}}\sum_b^{N^{\beta}}\left[J_{ab}^{\beta\beta} - K_{ab}^{\beta\beta}\right] + \sum_a^{N^{\alpha}}\sum_b^{N^{\beta}} J_{ab}^{\alpha\beta}. \tag{2}$$

In this expression, $h_{aa}^{\alpha} = \left\langle\psi_a^{\alpha}\middle|h_a\middle|\psi_a^{\alpha}\right\rangle$, $J_{ab}^{\alpha\beta} = \left\langle\psi_a^{\alpha}\middle|J_b^{\beta}\middle|\psi_a^{\alpha}\right\rangle = \left\langle\psi_b^{\beta}\middle|J_a^{\alpha}\middle|\psi_b^{\beta}\right\rangle = J_{ba}^{\beta\alpha}$, $J_{ab}^{\alpha\alpha} = \left\langle\psi_a^{\alpha}\middle|J_b^{\alpha}\middle|\psi_a^{\alpha}\right\rangle = \left\langle\psi_b^{\alpha}\middle|J_a^{\alpha}\middle|\psi_b^{\alpha}\right\rangle = J_{ba}^{\alpha\alpha}$, and $K_{ab}^{\alpha\alpha} = \left\langle\psi_a^{\alpha}\middle|K_b^{\alpha}\middle|\psi_a^{\alpha}\right\rangle = \left\langle\psi_b^{\alpha}\middle|K_a^{\alpha}\middle|\psi_b^{\alpha}\right\rangle = K_{ba}^{\alpha\alpha}$.

The Pople–Nesbet approach transforms the UHF equations into a matrix formulation by expanding $\psi_i^{\alpha/\beta}$ in a set of known basis functions $\{\phi_\nu|\nu = 1, \ldots, k\}$,

$$\psi_i^{\alpha/\beta} = \sum_\nu C_{\nu i}^{\alpha/\beta}\phi_\nu, \tag{3}$$

where the expansion coefficients $C_{\nu i}^{\alpha/\beta}$ become the parameters to be iterated. When equation (3) is inserted into equation (1) one obtains the characteristic $k \times k$ Pople–Nesbet coupled matrix equations,

$$\mathbf{F}^{\alpha/\beta}\mathbf{C}^{\alpha/\beta} = \mathbf{S}\mathbf{C}^{\alpha/\beta}\varepsilon^{\alpha/\beta}, \tag{4}$$

where $\mathbf{S}$ is the positive defined overlap matrix ($S_{\mu\nu} = \langle\phi_\mu|\phi_\nu\rangle$) of basis functions, $\mathbf{C}^{\alpha/\beta}$ are the expansion coefficient matrices whose columns describe each spatial orbital $\psi_i^{\alpha/\beta}$, $\varepsilon^{\alpha/\beta}$ are the diagonal matrices of the orbital energies $\varepsilon_i^{\alpha/\beta}$ and $\mathbf{F}^{\alpha/\beta}$ are the Fock matrices with respective elements given by

$$F_{\mu\nu}^{\alpha/\beta} = \int \mathrm{d}^3\mathbf{r}\,\phi_\mu^*(\mathbf{r})\,f^{\alpha/\beta}\phi_\nu(\mathbf{r}). \tag{5}$$

At this point it becomes convenient to introduce the charge density for the spin-up and spin-down electrons, defined as $\rho^{\alpha/\beta}(\mathbf{r}) = \sum_a^{N^{\alpha/\beta}}\left|\psi_a^{\alpha/\beta}(\mathbf{r})\right|^2 = \sum_\mu\sum_\nu P_{\mu\nu}^{\alpha/\beta}\phi_\mu(\mathbf{r})\phi_\nu^*(\mathbf{r})$, where the elements of the respective density matrices are $P_{\mu\nu}^{\alpha/\beta} = \sum_a^{N^{\alpha/\beta}} C_{\mu a}^{\alpha/\beta}C_{\nu a}^{\alpha/\beta *}$. Thus, one can define two new quantities: (i) the total charge density, $\rho^T(\mathbf{r}) = \rho^{\alpha}(\mathbf{r}) + \rho^{\beta}(\mathbf{r})$, that yields N when integrated over all space; (ii) the spin density, $\rho^S(\mathbf{r}) = \rho^{\alpha}(\mathbf{r}) - \rho^{\beta}(\mathbf{r})$, that yields $2M_S$ after integration over all space. This last fact shows that UHF wavefunctions are eigenfunctions of S_Z, but not necessarily of S^2. One can then define the total charge ($\mathbf{P}^T = \mathbf{P}^{\alpha} + \mathbf{P}^{\beta}$) and spin ($\mathbf{P}^S = \mathbf{P}^{\alpha} - \mathbf{P}^{\beta}$) density matrices for the system. The elements of the two Fock matrices are obtained as $F_{\mu\nu}^{\alpha/\beta} = T_{\mu\nu} + G_{\mu\nu}^{\alpha/\beta}$, where $T_{\mu\nu} = -\hbar^2/(2m)\langle\phi_\mu|\nabla^2|\phi_\nu\rangle$ and $G_{\mu\nu}^{\alpha/\beta} = e^2/\varepsilon\sum_\lambda\sum_\sigma\left[P_{\lambda\sigma}^T\langle\phi_\mu\phi_\sigma||\mathbf{r}_1 - \mathbf{r}_2|^{-1}|\phi_\nu\phi_\lambda\rangle - P_{\lambda\sigma}^{\alpha/\beta}\langle\phi_\mu\phi_\sigma||\mathbf{r}_1 - \mathbf{r}_2|^{-1}|\phi_\lambda\phi_\nu\rangle\right]$, with m and ε being the material effective mass and dielectric constant.

The self-consistency of this approach lies in the fact that both $\mathbf{F}$ and $\mathbf{P}$ depend on $\mathbf{C}$, while the coupling of spin-up and spin-down equations occurs since $\mathbf{F}^{\alpha}(\mathbf{F}^{\beta})$ depends on $\mathbf{P}^{\beta}(\mathbf{P}^{\alpha})$ through $\mathbf{P}^T$. The procedure of solving equation (4) is: (i) given a confinement potential, one specifies N and $\{\phi_\nu\}$; (ii) the integrations on $S_{\mu\nu}$ and $T_{\mu\nu}$ are performed; (iii) an initial guess is used for $\mathbf{P}^{\alpha/\beta}$ and $\mathbf{P}^T$, the two-electron integrals in $G_{\mu\nu}^{\alpha/\beta}$ are performed, and the Fock matrices are constructed; (iv) $\mathbf{F}^{\alpha/\beta}$ is diagonalized to obtain $\mathbf{C}^{\alpha/\beta}$ and $\varepsilon^{\alpha/\beta}$, and a new $\mathbf{P}^{\alpha/\beta}$ is formed; (v) this iteration is repeated until the desired convergence for E_0^{UHF} be reached. The Pople–Nesbet ground-state energy can be written as

$$E_0^{\mathrm{UHF}} = \frac{1}{2}\sum_\mu\sum_\nu\left[P_{\nu\mu}^T T_{\mu\nu} + P_{\nu\mu}^{\alpha}F_{\mu\nu}^{\alpha} + P_{\nu\mu}^{\beta}F_{\mu\nu}^{\beta}\right]. \tag{6}$$

UHF functions are not, in general, eigenstates of S^2 (only of S_Z); an estimation for the total spin expected values is found from [25]

$$\langle S^2\rangle_{\mathrm{UHF}} = \left(\frac{N^{\alpha} - N^{\beta}}{2}\right)\left(\frac{N^{\alpha} - N^{\beta}}{2} + 1\right) + N^{\beta} - \sum_a^{N^{\alpha}}\sum_b^{N^{\beta}}\left[\sum_\mu\sum_\nu C_{\mu a}^{\alpha *}C_{\nu b}^{\beta}S_{\mu\nu}\right]^2, \tag{7}$$

$$\langle S_Z\rangle_{\mathrm{UHF}} = \frac{1}{2}\sum_\mu\sum_\nu\left(P_{\nu\mu}^{\alpha} - P_{\nu\mu}^{\beta}\right)S_{\mu\nu}. \tag{8}$$

As an application of the Pople–Nesbet approach, we consider a QD with radius R_0 confined to an infinite spherical potential in the presence of a magnetic field $\mathbf{B} = (0, 0, B_0)$ and populated up to 40 electrons. Its single-particle Hamiltonian is

$$H_0 = \frac{\hbar^2}{2m}\left(\mathbf{k} + \frac{e}{\hbar c}\mathbf{A}\right)^2 + g\frac{\mu_B}{\hbar}\mathbf{B}\cdot\mathbf{S}, \tag{9}$$

where μ_B is the Bohr magneton, g is the bulk g-factor, and we use the symmetric gauge, $\mathbf{A} = (\mathbf{B}\times\mathbf{r})/2$. Using atomic units, $E_0 = e^2/(2a_0)$ for energy and $a_0 = \hbar^2/(m_0e^2)$ for length, the Hamiltonian H_0 can be written in the dimensionless form

$$H_0 = \frac{1}{\widetilde{m}}\frac{a_0^2}{R_0^2}\left[-\frac{1}{x^2}\frac{\partial}{\partial x}\left(x^2\frac{\partial}{\partial x}\right) + \frac{\mathbf{L}^2}{x^2} + \frac{R_0^2}{2l_B^2}(L_Z + \widetilde{m}gS_Z) + \frac{R_0^4}{4l_B^4}x^2\sin^2(\theta)\right], \tag{10}$$

where $\widetilde{m} = m/m_0$, $l_B = \sqrt{\hbar c/(eB_0)}$ is the magnetic length and $x = r/R_0$. Without magnetic field, the normalized spatial eigenfunctions of H_0 are given by

$$\phi_\nu(\mathbf{r}) = \left[\frac{2}{R_0^3}\frac{1}{[j_{l+1}(\alpha_{nl})]^2}\right]^{1/2} j_l(\alpha_{nl}x)\, Y_{l,m_l}(\theta,\phi). \tag{11}$$

The boundary condition at the surface, $r = R_0$ (or $x = 1$), determines α_{nl} as the nth zero of the spherical Bessel function $j_l(\alpha_{nl}x)$, while $Y_{l,m_l}(\theta,\phi)$ is the spherical harmonic.

The Hamiltonian for the electron–electron interaction in atomic units becomes $H_{ee} = (a_0/R_0)2/(\varepsilon\,|\mathbf{x}_1 - \mathbf{x}_2|)$, where the usual multipole expansion for $|\mathbf{x}_1 - \mathbf{x}_2|^{-1}$ is used in our calculations.

The spatial orbitals considered in $\psi_i^{\alpha/\beta}$ define six lowest energy shells ($1s$, $1p$, $1d$, $2s$, $1f$, $2p$) without magnetic field [26]. Thus, the index $\nu \equiv n, l, m_l$ can assume up to 40 (20 spin-up and 20 spin-down) possible values for those shells. Certainly, the magnetic field lifts both spin and orbital degeneracies. We consider a GaAs QD, a wide-gap semiconductor having $\widetilde{m} = 0.065$, $g = 0.45$ and $\varepsilon = 12.65$.

The inclusion of a magnetic field requires modifications on the UHF equations. The spin-independent linear and quadratic magnetic terms of equation (10) are easily added to the definition of h in both $f^{\alpha/\beta}$ and $T_{\mu\nu}$. However, the inclusion of the spin-dependent linear term ($\sim B_0S_Z$) to h in $f^{\alpha/\beta}$ requires decomposition of the kinetic matrix into $T_{\mu\nu}^{\alpha/\beta}$. Thus, under a magnetic field one should make the substitution $P_{\nu\mu}^T T_{\mu\nu} \Rightarrow P_{\nu\mu}^\alpha T_{\mu\nu}^\alpha + P_{\nu\mu}^\beta T_{\mu\nu}^\beta$ in E_0^{UHF} (equation (6)).

Another important detail refers to the orbital basis $\{\phi_\nu|\nu = 1,\ldots,k\}$ used. Instead of the exact spherical Bessel functions of equation (11), the radial part of each orbital is decomposed in a sum involving five Gaussians confined to the region $x \leqslant 1$, while the angular part is maintained as defined by the orbital symmetry, that is, the basis is

$$\phi_{n,l,m_l}(x,\theta,\phi) = N_{nl}(1-x)^n x^l \prod_{i=1}^{n-1}(\widetilde{\alpha}_{il} - x) \times \sum_{k=1}^{5} V_k e^{-D_k R_0^2 x^2} Y_{l,m_l}(\theta,\phi), \tag{12}$$

where N_{nl} is the normalization, the polynomial $(1-x)^n$ nulls functions at the boundary $x = 1$, the polynomial in x^l is required for $l > 0$ states at the origin $x = 0$, the product in $(\widetilde{\alpha}_{il} - x)$ nulls functions at the zeros $\widetilde{\alpha}_{il}$ of the respective spherical Bessel function transposed to the interval $0 \leqslant x \leqslant 1$, and the last sum involves the expansion into five Gaussians. Higher order expansion did not show any improvement in our results for $N \leqslant 40$. The Gaussian coefficients V_k and exponents D_k are determined for each value of R_0, by maximizing the superposition between equations (11) and (12). Once V_k and D_k are determined, we run the UHF code for a given value of R_0 and N, and find the parameters $C_{\nu i}^{\alpha/\beta}$ that better describe equation (3) and give the minimal energy in equation (6).

At last, we have calculated two quantities that will be used later in the description of our results. The first one is the QD chemical potential, which yields the energy difference between two successive ground states,

$$\mu_{\mathrm{dot}}(N) = E_0(N) - E_0(N-1). \tag{13}$$

The second one is the QD charging energy, which yields the energy cost to add an extra electron to the system,

$$E_{\mathrm{char}}(N) = E_0(N+1) - 2E_0(N) + E_0(N-1). \tag{14}$$

From these two last equations, one can also see that $E_{\mathrm{char}}(N) = \mu_{\mathrm{dot}}(N+1) - \mu_{\mathrm{dot}}(N)$.

We show in figure 1 the results of a UHF Pople–Nesbet calculation for a GaAs QD having $R_0 = 100$ Å, at zero magnetic field. In the left upper panel we have compared the non-interacting electron problem and the UHF results as function of QD occupation. The shell structure occurs for magic numbers $N = 2, 8, 18, 20, 34$ and 40. It is observed that the electron–electron interaction decreases (increases) the non-interacting ground-state energy when the occupation corresponds to a shell less (more) than half-filled. At exactly half-filled cases, $N = 5, 13, 27$ and 37, the interacting and non-interacting energies are approximately equal.

In the left bottom panel of figure 1 we show both QD chemical potential (left scale, equation (13)) and charging energy (right scale, equation (14)), where the respective values of E_0 are obtained from the unrestricted calculation presented in the left upper panel. Note that μ_{dot} linearly increases as the occupation increases inside a given shell. When such a shell is totally filled, there is an abrupt change in μ_{dot} indicating that the following shell starts its occupation. The higher the occupation, the more abrupt is the change. An anomalous behaviour seems to occur with the $2s$ shell, whose μ_{dot} value is larger than the $1f$ shell, which has higher energy. The charging energy is another form to verify not only the presence of shell structure in the spectrum, but also the validity of Hund's rule for the filling of such shells. In principle, E_{char} must present larger (smaller) peaks when the total (half) occupation of a shell is achieved. The first fact is due to the higher difficulty in adding an electron to a QD in a filled shell state, while the second one refers to Hund's rule, which states that electrons must be added to the system with their spin being parallel, until all possible orbitals inside a given shell be occupied, making the total energy of the system be decreased because of the maximized exchange contribution. However, some discrepancies are verified in E_{char}: the smaller peak of $N = 27$ occurs at $N = 26$, and the larger peak of $N = 20$ is negative.

The right bottom and upper panels of figure 1 show respectively the N-evolution of the total spin S and its

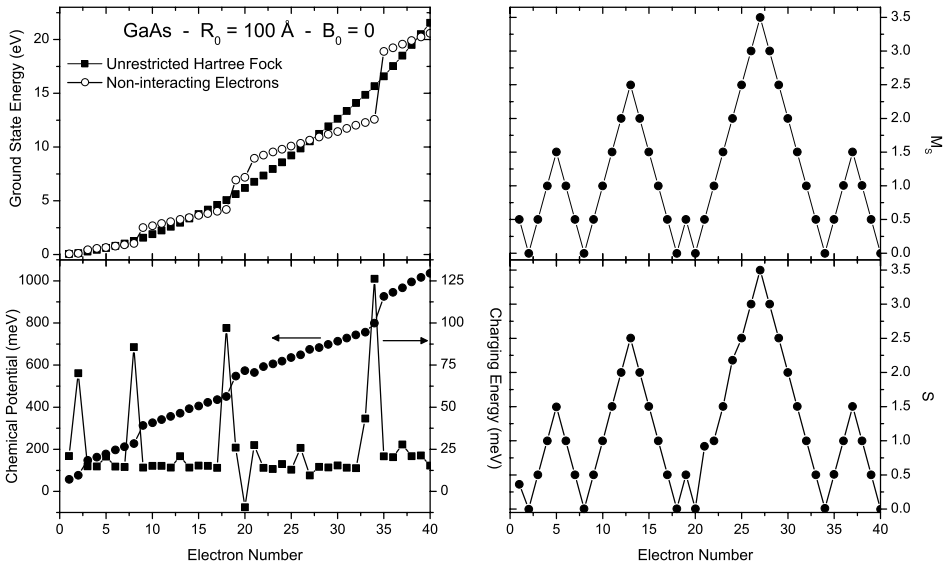

Figure 1. Unrestricted ground-state energies for a $R_0 = 100$ Å GaAs QD without magnetic field. In the left upper panel we compare UHF and non-interacting energies, where the QD energy shell structure is visible. The left bottom panel shows QD chemical potential (left scale) and charging energy (right scale). The former displays abrupt change always when a new shell starts to be filled, while the latter presents larger (smaller) peaks when a shell is fully (half) filled, a direct consequence of the Hund rule. The right bottom and upper panels show, respectively, the N-evolution of the expected values of total spin and its z-projection.

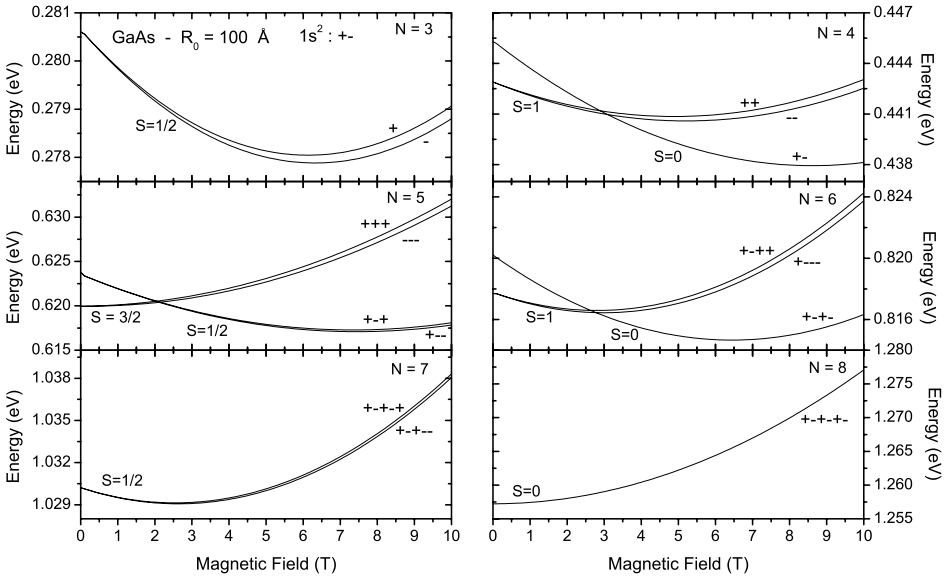

Figure 2. Violation of the Hund rule induced by magnetic field in the $R_0 = 100$ Å GaAs QD of the previous figure. Panels show successive occupation (indicated in the right upper corner) of the $1p$ shell, assuming that the $1s$ shell remains populated by one spin-up and one spin-down electron. The possible spin configurations for a given N are indicated by + (spin-up) and − (spin-down). At $B_0 = 0$ the spin sequence is $1/2 - 1 - 3/2 - 1 - 1/2 - 0$, while at fields higher than 3 T it changes to $1/2 - 0 - 1/2 - 0 - 1/2 - 0$. Energy triplets and quartets are suppressed by the field.

projection M_S as calculated from equations (7) and (8) for the unrestricted energies shown in the left upper panel. Note that, with no magnetic field, the Hund rule seems to be followed; the M_S expected value oscillates from 0 in a filled shell to its maximum in a half-filled shell, when it starts to decrease again on the way to the closing of the shell; the maxima are $M_S = 1/2, 3/2, 5/2$ and $7/2$ for s, p, d and f shells, respectively. The S expected value yielded by the unrestricted formalism is also very reasonable; discrepancies are only observed at $N = 24$, where $S > 2$, and at $N = 21$, where $S > 1/2$. We believe that both discrepancies related to the $2s$ shell or to its surroundings, $\mu_{\rm dot}$ larger than the one of $1f$ shell, negative peak for $N = 20$ in $E_{\rm char}$ and almost doubled S expected value for $N = 21$, are caused by the non-reasonable Gaussian reproduction of this orbital [27].

By focusing on the $1p$ shell we show in figure 2, for the same QD of the previous figure, how a finite magnetic field is able to violate the Hund rule in the system. Panels from left to right and from top to bottom show the successive ground-state energies from $N = 3$ to $N = 8$ as this shell is filled, always considering that the $1s$ shell remains fully occupied by two electrons, one spin-up and one spin-down; the distinct

possible spin configurations for each N are indicated by + (up) and − (down). In addition to the small Zeeman effect present in all occupations, there is a changing of ground-state spins at $N = 4, 5$ and 6 as the field is increased. Note that at zero field the spin sequence is $1/2 - 1 - 3/2 - 1 - 1/2 - 0$; in a field above 3 T (for the considered radius and material) it becomes $1/2-0-1/2-0-1/2-0$, meaning that quartets and triplets are suppressed by the magnetic field, and the ground state starts to oscillate only between singlets and doublets at high fields as N increases. When this $1p$ shell is half-filled ($N = 5$), the ground state goes from a quartet to a doublet at $B_0 \simeq 2$ T; when it has one electron more ($N = 6$) or less ($N = 4$) than that, it goes from a triplet to a singlet at $B_0 \simeq 3$ T. This same behaviour is expected to occur for every p shell.

At last, in order to prove the efficiency of the Pople–Nesbet approach, we compared the results from the UHF self-consistent matrix formulation with those obtained from the **LS**-coupling scheme used in [28], where a GaAs QD having $R_0 = 90$ Å was considered, and the quadratic term in B_0 was neglected since only small fields were considered; also, only $N = 2$ and $N = 3$ occupations were treated, since the states were exactly built (not only a single Slater determinant), and the electron–electron interaction was included by using perturbation theory, justified at such radius. At zero field the energies for $N = 2$ are 16.5 meV (**LS**) and 16.1 meV (UHF), while for $N = 3$ they are 34.8 meV (**LS**) and 33.9 meV (UHF); so, the formalism here used indeed gives smaller ground-state energies than the **LS** perturbative scheme. We have also checked the validity of neglecting the quadratic term in B_0 for fields smaller than 2 T. One should emphasize that a disadvantage of the UHF approach is that, in principle, it is not sure that one obtains trustable information about the L and S expected values of QD states; on the other hand, the applicability of the **LS** scheme is highly decreased as the QD occupation increases. Certainly, an extension for a CI (configuration interaction) calculation is necessary in order to account for correlation energies.

We have shown how the unrestricted Pople–Nesbet approach applied to a spherical QD under a magnetic field yields a reasonable description of its energetic spectrum, where a maximum occupation of 40 electrons has been considered. We have seen how both QD chemical potential and charging energy reproduce the filling and half-filling structures of the energy shells at zero field. With the total spin expected value for each occupation in a given radius, we have seen that the Hund rule is satisfied at zero field. However, under a finite field, we have shown that it is violated and, at given field values which depend on QD parameters, transitions that change ground-state symmetries are observed.

Acknowledgments

We acknowledge support from Brazilian agencies: FAPESP and CNPQ.

References

[1] Jaskólski W 1996 *Phys. Rep.* **271** 1
[2] Connerade J P, Dolmatov V K and Lakshmit P A 2000 *J. Phys. B: At. Mol. Opt. Phys.* **33** 251
[3] Rivelino R and Vianna J D M 2001 *J. Phys. B: At. Mol. Opt. Phys.* **34** L645
[4] Bielinska-Waz D, Karkowski J and Diercksen G H F 2001 *J. Phys. B: At. Mol. Opt. Phys.* **34** 1987
[5] Beekman R A, Roussel M R and Wilson P J 1999 *Phys. Rev.* A **59** 503
[6] Averin D V, Korothov A N and Likharev K K 1991 *Phys. Rev.* B **44** 6199
[7] Beenakker C W J 1991 *Phys. Rev.* B **44** 1646
[8] Grabert H 1991 *Z. Phys.* B **85** 319
[9] Kouwenhoven L P, van der Vaart N C, Johnson A T, Kool W, Harmans C J P M, Williamson J G, Staring A A M and Foxon C T 1991 *Z. Phys.* B **85** 367
[10] Weinmann D, Häusler W and Kramer B 1996 *Ann. Phys.* **5** 652
[11] Cipriani G, Rosa-Clot M and Taddei S 2000 *Phys. Rev.* B **61** 7536
[12] Jauregui K, Häusler W, Weinmann D and Kramer B 1996 *Phys. Rev.* B **53** R1713
[13] Harting J, Mülken O and Borrmann P 2000 *Phys. Rev.* B **62** 10207
[14] Pfannkuche D, Gudmundsson V and Maksym P A 1993 *Phys. Rev.* B **47** 2244
[15] Alhassid Y and Malhotra S 2002 *Phys. Rev.* B **66** 245313
[16] Reusch B and Grabert H 2003 *Phys. Rev.* B **68** 045309
[17] Bednarek S, Szafran B and Adamowski J 1999 *Phys. Rev.* B **59** 13036
[18] Ferconi M and Vignale G 1994 *Phys. Rev.* B **50** 14722
[19] Heiss W D and Nazmitdinov R G 1997 *Phys. Rev.* B **55** 16310
[20] Lozovik Y E and Volkov S Y 2003 *Phys. Sol. Stat.* **45** 364
[21] Sundqvist P A, Volkov S Y, Lozovik Y E and Willander M 2002 *Phys. Rev.* B **66** 075335
[22] Pandey R K, Harbola M K and Singh V A 2003 *Phys. Rev.* B **67** 075315
[23] Szafran B, Adamowski J and Bednarek S 1999 *Physica* E **4** 1
[24] Condon E U and Shortley G H 1977 *The Theory of Atomic Spectra* (London: Cambridge University Press)
[25] Szabo A and Ostlund N S 1999 *Modern Quantum Chemistry* (New York: Dover)
[26] Fetter A L and Walecka J D 1971 *Quantum Theory of Many-Particle Systems* (San Francisco: McGraw-Hill)
[27] Destefani C F, Vianna J D M and Marques G E *J. Phys. B: At. Mol. Opt. Phys.* (*Preprint* physics/0404007) (submitted)
[28] Destefani C F, Marques G E and Trallero-Giner C 2002 *Phys. Rev.* B **65** 235314